Motexafin-Gadolinium Taken Up *In vitro* by at Least 90% of Glioblastoma Cell Nuclei

Gelsomina De Stasio,[1] Deepika Rajesh,[2] Judith M. Ford,[5] Matthew J. Daniels,[1] Robert J. Erhardt,[3] Bradley H. Frazer,[1] Tolek Tyliszczak,[6] Mary K. Gilles,[6] Robert L. Conhaim,[4] Steven P. Howard,[2] John F. Fowler,[2] François Estève,[7] and Minesh P. Mehta[2]

Abstract

Purpose: We present preclinical data showing the *in vitro* intranuclear uptake of motexafin gadolinium by glioblastoma multiforme cells, which could serve as a prelude to the future development of radiosensitizing techniques, such as gadolinium synchrotron stereotactic radiotherapy (GdSSR), a new putative treatment for glioblastoma multiforme.

Experimental Design: In this approach, administration of a tumor-seeking Gd-containing compound would be followed by stereotactic external beam radiotherapy with 51-keV photons from a synchrotron source. At least two criteria must be satisfied before this therapy can be established: Gd must accumulate in cancer cells and spare the normal tissue; Gd must be present in almost all the cancer cell nuclei. We address the *in vitro* intranuclear uptake of motexafin gadolinium in this article. We analyzed the Gd distribution with subcellular resolution in four human glioblastoma cell lines, using three independent methods: two novel synchrotron spectromicroscopic techniques and one confocal microscopy. We present *in vitro* evidence that the majority of the cell nuclei take up motexafin gadolinium, a drug that is known to selectively reach glioblastoma multiforme.

Results: With all three methods, we found Gd in at least 90% of the cell nuclei. The results are highly reproducible across different cell lines. The present data provide evidence for further studies, with the goal of developing GdSSR, a process that will require further *in vivo* animal and future clinical studies.

Glioblastoma multiforme, the most common primary intracranial malignancy in the United States, has an annual incidence of ~12,000 cases; the incidence and mortality are equal, highlighting the almost uniformly fatal outcome of this disease and the need for new therapeutic approaches. The vast majority of glioblastoma multiforme patients succumb within 1 year of diagnosis. Current therapy consists of maximal resection followed by postoperative radiotherapy to ~60 Gy with temozolomide chemotherapy, with a median survival of just under 15 months (1). The brachytherapy and radiosurgery experience with this tumor suggests that the effective tumor control dose may possibly be in excess of 100 Gy, which is clinically not achievable in most patients today without inordinate morbidity. Although molecular biology-based therapy and chemotherapy are the major focus of current clinical research efforts, a more immediate effect could potentially be achieved by developing radiotherapy methods aiming to enhance dose delivery to cancer cells while sparing surrounding healthy tissues. Synchrotron stereotactic radiotherapy with gadolinium (GdSSR) could be one such novel approach. GdSSR consists of administering a tumor-specific Gd compound and subsequent stereotactic irradiation with monochromatic X-rays, at 51-keV photon energy from a synchrotron beamline. This energy is just above the Gd K-edge and therefore extracts electrons from the K-shell by photoelectric effect. The vacancy left behind by electron excitation and ejection is rapidly filled by fluorescence decay and by the Auger electron cascade from other shells. A similar idea, without the synchrotron monochromatic beam, has been described as photon activation therapy. In both cases, the emitted Auger electrons have high linear energy transfer and induce nonrepairable double-strand DNA breaks. However, the effective path length of the Auger electrons is extremely short; therefore,

Authors' Affiliations: [1]Department of Physics and Synchrotron Radiation Center, University of Wisconsin-Madison, Stoughton, Winconsin; Departments of [2]Human Oncology, [3]Statistics, and [4]Surgery, University of Wisconsin, Madison, Wisconsin; [5]Department of Radiation Oncology, University of California Los Angeles, Los Angeles, California; [6]Lawrence Berkeley National Laboratory, Berkeley, California; and [7]Institut National de la Sante et de la Recherche Medicale U647/Rayonnement Synchrotron et Recherche Médicale at European Synchrotron Radiation Facility and Unité Imagerie par Résonance Magnétique, Centre Hospitalier Universitaire, Grenoble, France

Received 4/4/05; revised 10/2/05; accepted 10/25/05.

Grant support: University of Wisconsin Comprehensive Cancer Center, UW-Graduate School Romnes Award, and Department of Physics. X-PEEM spectromicroscopy experiments were conducted at the UW-Synchrotron Radiation Center supported by the NSF grant DMR-0084402. The ALS and work on the beamline 11.0.2 STXM are supported by DOE-BES at LBNL under contract no. DE-AC03-76SF00098.

The costs of publication of this article were defrayed in part by the payment of page charges. This article must therefore be hereby marked *advertisement* in accordance with 18 U.S.C. Section 1734 solely to indicate this fact.

Requests for reprints: Gelsomina De Stasio, Department of Physics and Synchrotron Radiation Center, University of Wisconsin-Madison, 3731 Schneider Drive, Stoughton, WI 53589. Phone: 608-877-2000; Fax: 608-877-2001; E-mail: pupa@src.wisc.edu.

doi:10.1158/1078-0432.CCR-05-0743

such double-strand DNA breaks are possible only if Gd is localized in close proximity to DNA, which effectively requires either intranuclear or intramitochondrial localization.

Recent experiments with iodinated contrast agents and synchrotron radiation show that it is possible to enhance radiation lethality. This is due to the use of a synchrotron photon beam tunable to the optimal absorption energy of 34 keV (2, 3). Platinum compounds were also tested for SSR at 78.8 keV, resulting in a dramatic increase in DNA damage (4, 5). *In vivo* experiments in rats bearing F98 brain glioma showed the effectiveness of SSR using either iodine or platinum, both in stereotactic irradiation mode (6–8). In particular, outstanding results were obtained using intracranial infusion of *cis*-platinum 1 day before exposure to 78.8-keV photons (15 Gy single dose delivery) with a 34% survival rate at 1 year, which, to put things in context, is the best survival ever obtained in the F98 model (4). These data provide proof-of-principle evidence for SSR, using Pt or I, which have their absorption K-edges above and below the Gd K-edge, respectively. It is therefore expected that Gd will be equally effective as an SSR agent.

The advantage of GdSSR is principally the availability of newer Gd-containing experimental agents (such as motexafin gadolinium) that are administered i.v., and in early human clinical trials have shown tumor specificity and penetration with intratumor localization, corroborated with post-infusion resection, as well as imaging during a course of multiple administrations. In previous studies, we have shown that a Gd-containing compound can penetrate the plasma membrane of glioblastoma multiforme cells, *in vitro* and *in vivo*, and we have also shown higher Gd accumulation in the cell nucleus (relative to the cytoplasm) *in vitro*. These *in vitro* experiments were done on human glioblastoma multiforme cells in culture (TB10) exposed to Gd-diethylenetriaminepentaacetic acid (Gd-DTPA, Magnevist). Three independent techniques, Microscope à Emission de Photoélectrons par Illumination Synchrotronique de Type Onduleur (an instrument built by us which provides 20-nm optimum resolution), inductively coupled plasma-mass spectrometry (ICP-MS), and time of flight secondary ion mass spectrometry, all showed intracellular localization (9). We also tested the *in vivo* biodistribution of Gd-DTPA in six glioblastoma multiforme patients injected with Gd-DTPA before tumor excision. The tumor was frozen and sectioned for ICP-MS and Microscope à Emission de Photoélectrons par Illumination Synchrotronique de Type Onduleur analysis. We found evidence for Gd intracellular localization within the tumor in all six cases. However, Gd localized in only 6.1% of the cell nuclei analyzed. These data conclusively showed intracellular localization of Gd-DTPA, an observation not previously made, but also ruled out Gd-DTPA as a suitable sensitizer due to the limited number of cells in which it was taken up. However, those data did show (for the first time, to the best of our knowledge), that Gd, injected in the blood stream in the form of Gd-DTPA, not only reaches areas of blood-brain barrier breakdown but also a proportion of glioblastoma multiforme cells, penetrating the cell membrane and localizing within the nucleus (10). These observations were made possible because of the spatial resolution and chemical sensitivity of synchrotron spectromicroscopy, which enabled Gd evaluation at subcellular resolution, an approach not previously studied; we believe that the lack of such detailed analysis is the basis for the conventional wisdom that Gd-containing imaging agents do not penetrate intracellularly into glioblastoma multiforme.

To move the field forward, however, we needed a Gd-containing agent with greater likelihood of localization in the majority of tumor cells. A new experimental agent, motexafin gadolinium, is one such candidate (11–14). Motexafin gadolinium, a tripyrrolic pentadentate aromatic metallotexaphyrin, is a redox mediator that selectively reaches tumor cells and produces reactive oxygen species (15). Our group and others have previously published data showing the tumor-specific and prolonged retention of motexafin gadolinium in brain metastases and glioblastoma multiforme (16, 17). Prolonged and preferential accumulation and retention of motexafin gadolinium has now also been shown in the phase I and II trials of this agent as a radiosensitizer for glioblastoma multiforme (18).

The fraction of cancer cells taking up intranuclear Gd remains the major variable limiting the success of GdSSR, and this will be a function of the tumor specificity of various Gd-containing compounds. An assessment of this variable is therefore a prerequisite to the clinical testing of any Gd compound for use in GdSSR, and the current article reports our first experiments with motexafin gadolinium to determine this localization variable *in vitro*. We analyzed the intranuclear distribution of Gd in four human glioblastoma multiforme cell lines after exposure to motexafin gadolinium. The results are reproduced and corroborated with three different microscopy techniques: X-ray photoelectron emission spectromicroscopy (X-PEEM), scanning transmission X-ray microscopy (STXM), and confocal fluorescence microscopy. Intranuclear localization was used as an end point because of the short path length of the emitted Auger electrons. The best energy for GdSSR is calculated to be 51 keV (6). Auger electrons emitted by Gd atoms, under X-ray illumination at 51 keV, range in energy between 0 and 41 keV with an average of 7.63 keV (19) and average linear energy transfer of 0.3 MeV/μm (10). The radiation length (or mean inelastic path) of Auger electrons is limited to less than 150 nm (15 nm for the average energy of 7.63 keV; refs. 19, 20). Due to this rather short path length of Auger electrons, it is necessary for Gd atoms to be localized in the immediate proximity of DNA (i.e., within the nucleus or in the mitochondria; refs. 9, 10). When an Auger electron is emitted, it most likely will interact with water molecules within a radius of a few nanometers, producing hydroxyl radicals, which in turn locally propagate the oxidative damage (21). Lethal double-strand DNA breaks occur in proportion to the extent of the radiation-induced oxidative damage. Hence, determining how many cell nuclei contain Gd in a tumor is fundamental for the success of GdSSR.

Materials and Methods

Cell culture and exposure to motexafin gadolinium. We used four well-established human glioblastoma multiforme cell lines: T98G (22), U87 (23), MO59K (24), and TB10 (9, 25). Cells were grown on precut 10 mm × 10 mm silicon wafers (Silson, Northhampton, United Kingdom) for X-PEEM spectromicroscopy; on 1 mm × 1 mm Si_3N_4 windows, 100 nm thick (Silson) for STXM spectromicroscopy; on tissue culture-treated polystyrene slides for confocal microscopy; and in Petri dishes for ICP-MS analysis. Subconfluent cultures were exposed to motexafin gadolinium (Pharmacyclics, Sunnyvale, CA), formulated at

2.3 mg/mL in 5% aqueous mannitol, and added to the culture medium to a final concentration of 100 μmol/L. Six different exposure times ranging from 0 to 72 hours were used for the ICP-MS time course measurements. For all microscopy experiments exposure times were kept constant at 72 hours. The cell appearance was not altered by motexafin gadolinium exposure.

During the culture and exposure periods, all cell lines were maintained in a humidified incubator at 37°C and grown in DMEM/F12 medium containing 10% fetal bovine serum, 1% penicillin and streptomycin, and 1% nonessential amino acids (all from Mediatech, Herndon, VA).

After exposure to motexafin gadolinium, the cell cultures on Si substrates for X-PEEM analysis were washed thrice with PBS solution to remove free Gd, fixed in 4% paraformaldehyde in PBS for 20 minutes, double-washed in Milli-Q-water, and air dried. At this point, some cell cultures were sputtered with 3-kV argon ions at 10^{-5} Torr for 10 minutes; others were not. Sputtering removes the topmost portion of the cell to reveal the inner nuclear compartment of fixed cells (26). Sputtered and unsputtered cells were then ashed in UV/O_3 for 140 hours (27). Parallel cultures were run and treated identically for ICP-MS measurements of the bulk Gd concentration. Cell cultures for STXM analysis on Si_3N_4 windows, after motexafin gadolinium exposure, were washed, fixed, washed, and air-dried. Cell cultures for confocal microscopy were grown on a slide flask (Nunc, Rochester, NY) containing a tissue culture–treated polystyrene slide. They were allowed to adhere for 24 hours and then exposed to 100 μmol/L motexafin gadolinium for 72 hours. The upper flask structure was then snapped away, and the cells were washed, fixed with 4% paraformaldehyde in PBS, washed, and air-dried. The slides were mounted with ProLong Antifade (Molecular Probes, Eugene, OR) and imaged with confocal microscopy. Each sample was prepared in duplicate, triplicate, or quadruplicate.

ICP-MS analysis. Cell cultures for ICP-MS bulk [Gd] analysis, after exposure, were washed, digested in 1 mL of 1 N HNO_3, and scraped from the Petri dishes with a plastic spatula. The number of cells in each culture, typically 2 to 20 × 10^5 per sample, was measured from a small aliquot. The total cell volume was then calculated, knowing the average volume of cells for each cell line. These were measured across six separate samples for each cell line, giving the following mean results: 62,400 TB10 cells/μL, 74,400 T98G cells/μL, 15,000 MO59K cells/μL, and 9,200 U87 cells/μL. Once the accurate cell volume in each motexafin gadolinium-exposed sample was obtained using these numbers, the ICP-MS results could be normalized (typical volume of cells, 10-40 μL/sample). This strategy gave reproducible results across two repeated cultures, with errors usually within 25% (Fig. 1).

Tissue samples from three glioblastoma multiforme patients were also analyzed with ICP-MS (Table 1). These were collected from glioblastoma multiforme tissue and plasma for patients 1 and 2, and from tumor necrotic and uninvolved brain areas for the postmortem patient 3. All [Gd] were normalized to the measured tissue weight and volume.

X-PEEM spectromicroscopy analysis. X-PEEM spectromicroscopy analysis was done using the Spectromicroscope for PHotoelectron Imaging of Nanostructures with X-rays (SPHINX) instrument (Elmitec GmbH, Clausthal, Germany), installed on the HERMON beamline at the Synchrotron Radiation Center (Madison, WI). SPHINX has an optimum lateral resolution of 10 nm (28) and acquires X-ray absorption spectra with a resolving power up to 15,000 ($E/\Delta E$) in the 60 to 1,300 eV energy range. Phosphorus distribution maps were acquired to localize the nucleus in each cell. These were obtained by digital ratio of images at 139 and 132 eV, on-peak and pre-peak of the P2p edge (29). For trace concentration Gd analysis, we extracted Gd location maps as described previously (10, 28, 29), at the Gd3d edge (also known as M-edge at ~1,183 eV). In such Gd maps (Fig. 2), binned 4 × 4, the resolution is four times lower than in the images, and the Gd pixel size = 1.4 × 1.4 = 2 μm^2. In these maps, Gd pixel color corresponds to Gd concentration (peak area). Because an absolute calibration is not yet available, only information about relative concentrations is obtained. From the ICP-MS results of Fig. 1 and many other reference standards, we estimate that this spectromicroscopy trace element analysis has a minimum detection limit of <1,000 ppm. Cell and tissue ashing increases [Gd] by a factor of 10; therefore, the detection limit was on the order of ≤100 ppm in all cells analyzed here. In our analysis, we accepted one Gd-containing pixel per cell nucleus as sufficient to count that cell as one with a Gd-containing nucleus (29).

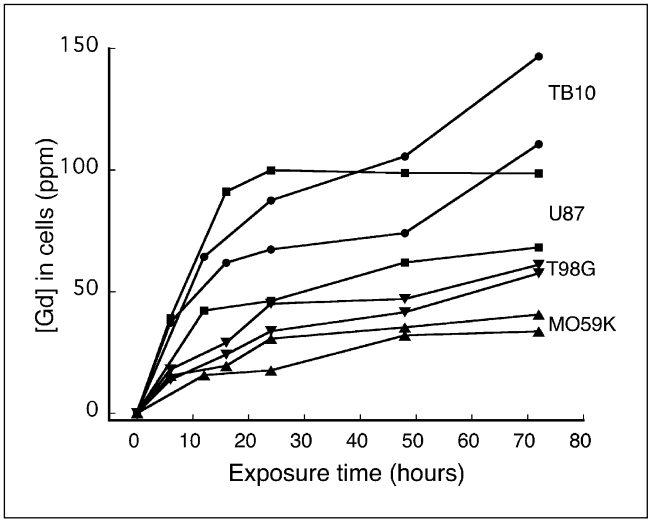

Fig. 1. Time dependence of Gd uptake in TB10 (●), U87 (■), T98G (▼), and MO59K (▲) human glioblastoma multiforme cell lines. Two independent cell cultures per cell line were exposed to 100 μmol/L motexafin gadolinium (16 ppm Gd) for 0 to 72 hours, and the [Gd] in cells was measured by ICP-MS.

Ashing in UV/O_3 selectively removes carbon, a major element in cells and tissues, and consequently enhances the relative concentration of the other elements. Ashing takes place at air pressure and temperature and slowly (100-200 hours) "flattens" the cell morphology. It is particularly useful when the element to be localized by spectromicroscopy is present in trace concentrations; otherwise, it is undetectable (27).

In the SPHINX experiments reported here, we identified the cell nuclei from the P distribution map in 180 TB10 cells and counted the number of cell nuclei containing at least 1 Gd pixel, evaluated the effectiveness of motexafin gadolinium in reaching glioblastoma multiforme nuclei.

STXM spectromicroscopy analysis. The STXM instrument on beamline 11.0.2 at the Advanced Light Source in Berkeley uses an undulator source and is optimized for the Gd3d absorption energy. This spectromicroscope (30, 31) is both faster and more sensitive than X-PEEM for Gd detection. Ashing of the cell cultures for STXM analysis, therefore, was not required. We analyzed three cell cultures, containing 34 T98G cells, 27 MO59K cells, and 139 TB10 cells, respectively. For Gd detection in cells, we acquired images on-peak and off-peak, at 1,183 and 1,178 eV; the ratio of these two images provided a Gd distribution map. Although this instrument does not allow the detection of P for identification of nuclei, cell nuclei seem thicker and denser in transmitted X-rays, and their outline can easily be visualized, allowing adequate scoring of Gd uptake.

Confocal microscopy. Three of the four cell lines (TB10, MO59K, and T98G) were analyzed using a Bio-Rad (Richmond, CA) MRC 1024ES confocal microscope. This instrument can simultaneously measure the fluorescence from three channels, with excitation wavelengths from the three lines of a krypton/argon laser and emission through three independent barrier filters. These are 568 and 585 nm (rhodamine channel); 488 and 522 nm (FITC channel), and 488 and 680 nm (Cy 5 channel). The most intense fluorescence signal from motexafin gadolinium–treated cells was observed in the rhodamine channel; therefore, all images were recorded only with the 568 to 585 nm settings.

Table 1. Intratumor (GBM) Gd measurements

Patient 1			Patient 2			Patient 3 (autopsy)	
Time	**Source**	**[Gd] ppm**	**time**	**Source**	**[Gd] ppm**	**Source**	**[Gd] ppm**
Pre	Plasma	0.0003	pre	Plasma	0.0021	Tumor	8.542
5 min	Plasma	12.973	5 min	Plasma	14.043	Tumor	8.022
45 min	Plasma	7.349	45 min	Plasma	8.143	Necrosis within tumor	2.144
2:30 hrs	Plasma	3.415	45 min	Tumor	22.589	Uninvolved brain area	0.216
2:30 hrs	Tumor	7.266	1:11 hrs	Tumor	29.728	Uninvolved brain area	0.126
3 hrs	Plasma	4.079	1:14 hrs	Plasma	6.536	Uninvolved brain area	0.068
3 hrs	Tumor	2.475	1:18 hrs	Tumor	19.580	Uninvolved brain area	0.143
24 hrs	Plasma	1.700	1:30 hrs	Plasma	6.309	Uninvolved brain area	0.109
			3 hrs	Plasma	5.109	Uninvolved brain area	0.064
			24 hrs	Plasma	1.770		

NOTE: Gd concentrations measured with ICP-MS. GBM patients 1 and 2 were injected with a single dose of MGd (10 mg/kg), before tumor resection. Patient 3 died 57 days after the last of multiple MGd doses, and the autopsy data are also reported.

The aperture was set for minimal optical section thickness, and laser power and photodetector gain were set to optimally image cell fluorescence within the 8-bit grayscale range of the photodetector. Five consecutive optical sections were obtained vertically through the cells to verify that motexafin gadolinium fluorescence originated from the nucleus and not only from the cytoplasm above or below the nucleus.

Magnetic resonance imaging. Magnetic resonance images (MRI) from one glioblastoma multiforme patient participating in a clinical trial of motexafin gadolinium and conventional radiotherapy at the University of California at Los Angeles (Protocol "A phase I dose escalating study of the safety and tolerability of gadolinium texaphyrin as a radiation sensitizer in patients with primary Glioblastoma Multiforme," University of California at Los Angeles Institutional Review Board approval no. 97-09-042). The patient was injected with 4 mg/kg motexafin gadolinium five times per week, then thrice per week, up to 13 doses. T_1-weighed MRIs were obtained immediately after 1, 5, and 13 doses. We also collected images 7 days after the last dose, to prove the long-term, intracellular retention of this drug.

Results

In Fig. 1, we report the ICP-MS results obtained on the four human glioblastoma cell lines. These results show total uptake of Gd in cells, irrespective of Gd location within the cell. The concentration of Gd after a 72-hour exposure to motexafin gadolinium varies slightly across the cell lines. Using the Student *t* test, [Gd] in TB10 cells is revealed to be significantly greater than in MO59K and T98G cells; [Gd] in T98G is also significantly greater than in MO59K; the other differences are not significant. The molecular mechanistic explanation for this phenomenon is currently not known, but the unifying observation across the four cell lines is that they all take up motexafin gadolinium intracellularly and concentrate it with respect to the exposure solution. The 100 μmol/L motexafin gadolinium exposure solution, in fact, contained 16 ppm Gd, whereas the concentration in cells varies between ~40 and ~120 ppm after a 72-hour exposure to motexafin gadolinium. The intracellular [Gd], therefore, is 2.5 to 7.5 times greater than the extracellular [Gd].

An additional uniform observation across all four cell lines is that the concentration of Gd increases with duration of exposure to motexafin gadolinium and exceeds the exposure solution concentration after the first 6 hours. Although the intracellular [Gd] continues to increase beyond 6 hours, the rate of increase diminishes after 12 hours, as shown by the decrease in slope for all four cell lines. Figure 1 summarizes these results.

The absolute concentration of Gd in cells, however, does not provide sufficient evidence that Gd is present intranuclearly. The subcellular localization of Gd cannot be assessed by ICP-MS but can be resolved by spectromicroscopic methods. We analyzed 180 randomly selected TB10 cells from three separate samples with the SPHINX spectromicroscope and found that 90% of them (162) contained at least one Gd pixel in the nucleus. In Fig. 2, we show a Gd location map representative of this analysis.

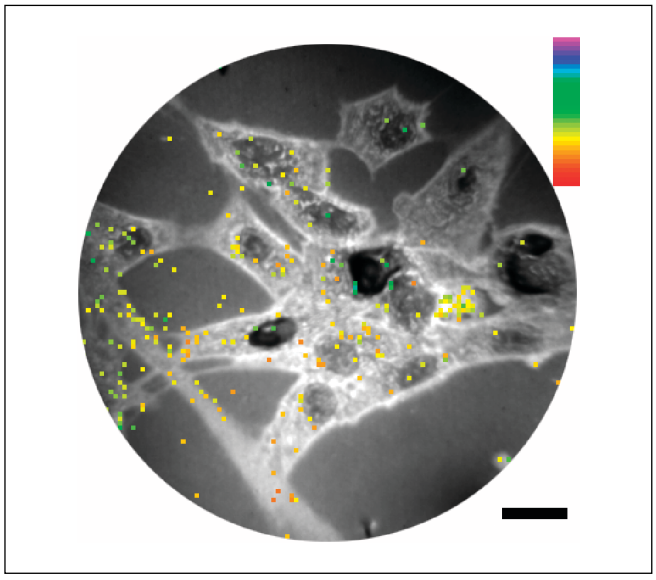

Fig. 2. SPHINX Gd location map in TB10 cells exposed to 100 μmol/L motexafin gadolinium for 72 hours and ashed. Each Gd pixel is 2 μm^2 and displayed in spectrum colors. The color bar indicates maximum [Gd] in magenta and minimum in red. The Gd location map is superimposed on a SPHINX grayscale image of the cells acquired at 144 eV. In this map, orange, yellow, and green Gd pixels are present in the cells, indicating medium or low Gd concentrations. No pixel indicates undetectable Gd. Several Gd pixels are present on the substrate. Bar, 20 μm.

We also noticed that some Gd pixels appear on the silicon substrate, where no cellular structures are visible. This result is peculiar to motexafin gadolinium and was not observed with other Gd compounds (e.g., Gd-DTPA or Gd-1,4,7,10-tetraazacylododecane-*N*,*N*[*N*′,*N*″,*N*‴-tetraacetic [Gd-DOTA]; see ref. 10). Motexafin gadolinium was observed on the substrate with all three microscopies used in the present experiments.

Of the 180 TB10 cells analyzed, 72 were sputtered and 108 were unsputtered. Of these, 63 and 99 cells, respectively, contained Gd. The change in percentage of Gd-containing nuclei with sputtering, from 92% before sputtering to 88% after sputtering, is not significant, indicating that Gd detected in the nucleus was mostly intranuclear and not deposited on the cell surfaces and removed by sputtering. In all cell cultures, Gd pixels also appear in the cytoplasm at higher densities than in the nuclei. Some of the cells in Fig. 2 indicate this behavior as well. It is possible that more cells contain Gd at a concentration below the SPHINX detection limit. We therefore analyzed other motexafin gadolinium–exposed cell cultures with the more sensitive STXM spectromicroscope. Figure 3 shows representative STXM results.

In the STXM Gd maps, we observe that Gd is distributed inhomogeneously in cells. It seems most intense in spots on the order of 1 μm in size, and these are denser around the nuclei than in the nuclei. These spots are very similar in size, density, and distribution to the Gd pixels observed with SPHINX. They are also denser around the nuclei than in the nuclei.

Overall, we analyzed 34 randomly selected T98G cells, 27 MO59K cells, and 139 TB10 cells with STXM. Thirty-one (90%) of the T98G cells contained Gd; 26 of the MO59K (96%), and 122 of the TB10 cells (88%) contained Gd in their nuclei. Although ICP-MS had indicated that motexafin gadolinium uptake in TB10 cells is significantly greater than in T98G or MO59K, we now know that the percentage of nuclei taking up Gd is not significantly different between these cell lines (see confocal results below). We, therefore, combined the results and found that, overall, 90% of the cells analyzed with STXM (including T98G and TB10) had at least one Gd pixel in their nuclei. This result confirms and verifies with higher sensitivity the intranuclear presence of Gd already observed with SPHINX.

Although the results from the two spectromicroscopic techniques very strongly suggest intranuclear localization of Gd from motexafin gadolinium, there is one possible confounding variable. If Gd were present in high concentration in the cytoplasm and absent from the nuclei, the small portion of cytoplasm above and below the nucleus could be mistaken for the nucleus in the transmission STXM experiment. Similarly, in the SPHINX experiment, Gd above the nucleus before ashing could seem to be localized in the nucleus after ashing and flattening of the cells. The sputtering of cells removes this as a source of error, and our results on sputtered cells analyzed with SPHINX indicate that Gd was truly intranuclear in location.

To further validate intranuclear localization using techniques that require less manipulation of cells, we analyzed motexafin gadolinium–exposed cells with confocal microscopy. The motexafin gadolinium molecule is fluorescent due to the extended texaphyrin aromatic system surrounding the Gd atom (32). Motexafin gadolinium–treated cells emit fluorescence photons in both the FITC and the rhodamine spectral regions, as shown in Fig. 4. However, because the emission intensity in the rhodamine region is higher and does not interfere with autofluorescence, we analyzed all cells in this spectral range (Fig. 5). The motexafin gadolinium–related fluorescence intensity observed with confocal microscopy is always higher

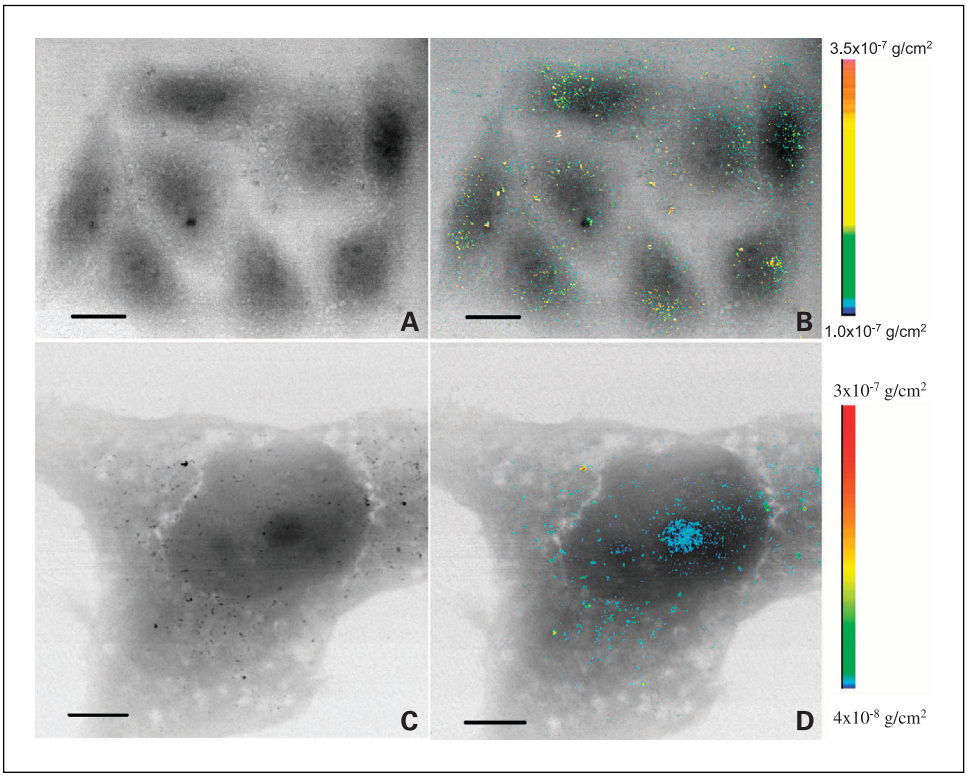

Fig. 3. STXM results on T98G (*A* and *B*) and TB10 cells (*C* and *D*) exposed to 100 μmol/L motexafin gadolinium for 72 hours. Images acquired at 1,183 eV (*A* and *C*) and Gd distribution maps (*B* and *D*) obtained by ratio of two images, at 1,178 and 1,183 eV. The spectrum colors correspond to Gd planar concentration, estimated by comparison with absorbance of known Gd thicknesses. Bars, 20 μm (*A* and *B*) and 5 μm (*C* and *D*).

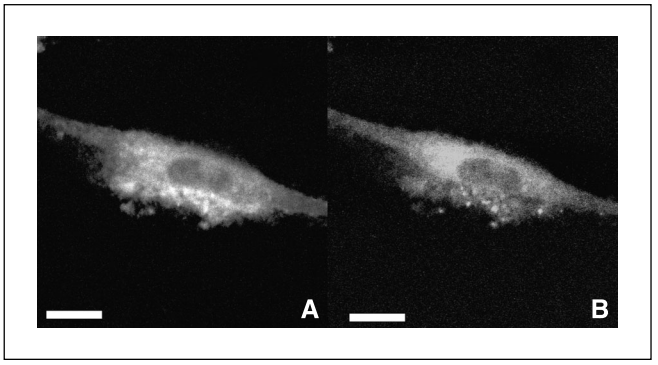

Fig. 4. Confocal fluorescence micrographs of a TB10 cell exposed to 100 μmol/L motexafin gadolinium for 72 hours. *A,* motexafin gadolinium – associated fluorescence imaged using 488-nm excitation and a 522-nm barrier filter (as for FITC fluorescence). *B,* motexafin gadolinium – associated fluorescence imaged using 568-nm excitation and a 585-nm barrier filter (as for rhodamine fluorescence). Bar, 20 μm.

from the cytoplasm than from the nucleus. This result confirms the same observation previously made with SPHINX and STXM. All control cell cultures not exposed to motexafin gadolinium were imaged using the same wavelengths and showed no fluorescence or autofluorescence. In all motexafin gadolinium – exposed cells imaged with confocal fluorescence microscopy, as with SPHINX and STXM, we observed higher intensity from perinuclear spots, ≤1 μm in size, which could be interpreted as subcellular organelles preferentially taking up motexafin gadolinium, as suggested by Woodburn (32), or simply aggregates of motexafin gadolinium.

Most importantly, optical slicing across the cell thickness unequivocally shows that motexafin gadolinium fluorescence originates from within the cell nuclei. We analyzed a total of 481 motexafin gadolinium – treated cells with confocal microscopy and found that 100% of them exhibited motexafin gadolinium – related fluorescence in cytoplasm and nuclei. None of the 143 control cells revealed fluorescence.

In Table 1, we report the raw data acquired by ICP-MS of [Gd] in glioblastoma multiforme patients injected with a single dose of motexafin gadolinium at 10 mg/kg.

Patients 1 and 2 had minimal MRI enhancement with this single dose of motexafin gadolinium. Much greater MRI enhancement in glioblastoma multiforme is achieved with repeated daily dosing. Repeating motexafin gadolinium doses may therefore be the best strategy for future clinical trials. The autopsy data on patient 3 indicate that the average tumor/normal tissue ratio is on average 70:1 (varying between 37 and 133), almost 2 months after treatment with multiple doses. This observation speaks to the tumor specific uptake and prolonged retention of Gd within glioblastoma multiforme using motexafin gadolinium as a delivery vehicle. Necrotic tumor shows 10- to 33-fold greater [Gd] compared with uninvolved normal brain.

Prolonged and preferential accumulation and retention of motexafin gadolinium in glioblastoma multiforme, as well as enhancement with repeated administration was also shown in the phase I and II trials of this agent as a radiosensitizer for glioblastoma multiforme (33). Figure 6 shows enhancement in MRI and retention after multiple injections of motexafin gadolinium.

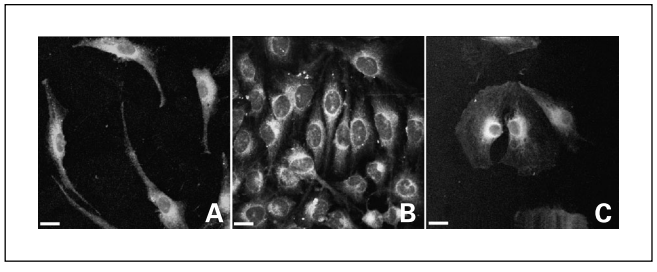

Fig. 5. Confocal microscopic images of motexafin gadolinium – related fluorescence from TB10 (*A*), T98G (*B*), and MO59K cells (*C*), exposed to 100 μmol/L motexafin gadolinium for 72 hours. All images are optical sections at the half-height of the cells. Bar, 20 μm.

Discussion

Goorley and Nikjoo calculated and compared the theoretical effectiveness of three different cancer therapy approaches based on gadolinium: neutron capture, radioisotope decay, and photon activation therapy. Their results indicate that of the three cases, the photoelectric event has the highest Auger electron yield and the highest amount of energy deposited in a 10 μm sphere, making it more effective at killing the cell in which the reaction takes place (19). Theoretically, tremendous improvement could be achieved if, as addressed here, Gd atoms and photoelectric events occur within the nuclei of cancer cells.

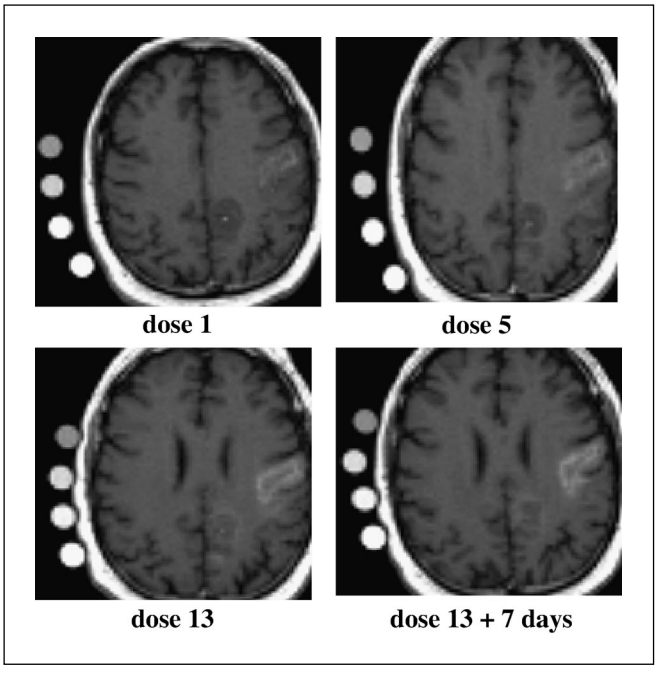

Fig. 6. T_1-weighed MRIs obtained after a first dose of 4 mg/kg motexafin gadolinium (*top left*) with no conventional contrast, after completing a 1-week, 5-dose loading course (*top right*), after completion of all 13 doses, given over a total of 3 weeks (*bottom left*) and 7 days after the 13th motexafin gadolinium injection (*bottom right*). The tumor (glioblastoma multiforme) is clearly visualized on all four noncontrast post-motexafin gadolinium images. Notice tumor specificity without normal brain parenchyma enhancement and the increase in tumor enhancement with increasing doses of motexafin gadolinium. Four external reference tubes, used for calibration, are also imaged. These contained 0.01, 0.05, 0.1, and 0.2 mg/mL motexafin gadolinium, respectively.

How much Gd in the nucleus is necessary for GdSSR? To address this question some calculations are necessary. We note that a single Gd photoabsorption event and consequent emission of Auger electrons close to DNA would kill a cell by inducing nonrepairable double-strand DNA breaks. However, sufficient Gd must be present in the nucleus of the majority of malignant cells in the tumor. The number of Gd photoabsorption events per cell nucleus (N) is obtained from the following formula:

$$N = n\Phi\mu$$

in which n = number of Gd atoms per nucleus; Φ = photon fluence = 10^8 photons/mm^2 s $\times$ 5 minutes = 3×10^{10} photons/mm^2, which is clinically acceptable, and corresponds to a dose of $\sim$20 Gy (4); and μ = absorption coefficient for gadolinium at 51 keV = 4.5×10^3 barn = 4.5×10^{-19} mm^2. For reference, the μ for carbon at the same energy is 0.19 barn (34). We add that at 51 keV photoabsorption from a K-shell electron occurs with 82% probability, and 18% from L-shell (19), generating 8.05 Auger electrons, with an average energy of 7.63 keV. The same photoabsorptions also generate the emission of two fluorescence photons, with average energy 34.9 keV (19). The Auger electrons, therefore, are the most abundant and also the most radiobiologically relevant particles, having the highest linear energy transfer (0.3 MeV/μm). Using the above formula, we calculate that one photoabsorption per nucleus can be achieved if 10^8 Gd atoms/nucleus are present, which corresponds to a [Gd] on the order of 10 ppm.

For GdSSR *in vivo*, assuming a Gaussian distribution of Gd molecules in cell nuclei as a result of uptake from the vasculature, Poisson statistics dictates that there must be an average of at least 24 Gd photoabsorption events per nucleus ([Gd] on the order of 100 ppm), to be sure that <1 in 10^{10} cells has zero events. That is, less than one cell per tumor must have zero photoabsorptions. This calculated [Gd] in nuclei is comparable, within one order of magnitude, with the detection limit of spectromicroscopy and with the measured Gd concentrations reported *in vitro* (Fig. 1) and *in vivo* (Table 1).

The observation of a 70:1 tumor/normal tissue ratio almost 2 months after treatment shows the tumor-specific uptake and prolonged retention of Gd within glioblastoma multiforme using motexafin gadolinium as a delivery vehicle. These data are particularly valuable as they show almost negligible Gd uptake in normal brain, an observation that is key to the success of GdSSR, as only a large differential in [Gd] between tumor and normal brain would make this therapeutic approach feasible. Significantly, even necrotic tumor shows 10- to 33-fold higher [Gd] compared with uninvolved brain areas.

Figure 6 shows the finding that much greater MRI enhancement in glioblastoma multiforme is achieved with repeated daily dosing with motexafin gadolinium than with a single dose, suggesting that repetitive motexafin gadolinium dosing may perhaps be the best strategy for future clinical trials.

If the concentration and/or distribution of Gd or the photon flux at 51 keV are lower, or Gd is inhomogeneously distributed across nuclei, tumor recurrence will not be avoided but may be slowed down. Consequently, the larger the number of nuclei a candidate Gd compound reaches, the greater its potential for GdSSR to slow down or cure glioblastoma. We recently analyzed glioblastoma multiforme cells *in vitro* exposed to two MRI contrast agents, Gd-DTPA and Gd-DOTA, as well as glioblastoma multiforme tissues from rat and human patients, after injection of the same two Gd compounds. We found that both of these compounds reach 84% and 56% of the nuclei *in vitro* and much less *in vivo* (down to 6.1% of 2,217 nuclei from human glioblastoma multiforme tissue sections; ref. 10).

In our quest for appropriate GdSSR agents, we have now analyzed the ability of motexafin gadolinium to localize intranuclearly in glioblastoma multiforme cells. We used three different experimental approaches (Figs. 2–5) to directly observe motexafin gadolinium in the nuclei of glioblastoma multiforme cells. With SPHINX, we found that the percentage of nuclei containing Gd is 90% (n = 180), with STXM it is 90% (n = 200), whereas with confocal microscopy, it is 100% (n = 481). STXM is more sensitive than SPHINX but did not yield Gd in a greater percentage of nuclei. Because with confocal microscopy we found 100% of the nuclei exhibiting motexafin gadolinium-related fluorescence, we conclude that this is the most sensitive probe among the three used. Fluorescence microscopy techniques cannot be used for the majority of Gd compounds, because these are not fluorescent. However, for motexafin gadolinium, fluorescence detection is a feasible approach.

Spectromicroscopic analysis, although slightly less sensitive than confocal fluorescence microscopy, is still necessary to provide definitive evidence of intranuclear Gd presence, because fluorescence emission originates from the aromatic, expanded porphyrin component of the motexafin gadolinium molecule and not from the Gd atom itself (32). It is conceivable that if the molecule is metabolized by the cell after uptake, the texaphyrin is still present, whereas the Gd^{3+} ion is actively eliminated from the intracellular and/or intranuclear compartments. The motexafin gadolinium molecule was designed to be extremely stable in solution. In contrast to the gadolinium chelates (e.g., Gd-DTPA, Gd-DOTA, etc.) previously described in the literature, in motexafin gadolinium, the gadolinium is held within its texaphyrin macrocyclic core by coordinate covalent bonds (11, 12, 32). It is therefore unlikely that motexafin gadolinium would be denatured in solution but could be actively metabolized by the cell. That is why we always referred to "motexafin gadolinium–related fluorescence," and not "motexafin gadolinium fluorescence" when describing the confocal data. It is possible that intracellularly, a motexafin gadolinium metabolite generates the detected fluorescence signal. Definitive proof of Gd presence, therefore, must be obtained with a direct elemental Gd probe. SPHINX and STXM analyses provide direct evidence and confirm intranuclear Gd presence in at least 90% of glioblastoma multiforme cells from four different cell lines exposed to motexafin gadolinium for 72 hours.

Our results are consistent with Woodburn's observations (32): she finds that extending exposure times to motexafin gadolinium results in increasing the number of nuclei taking up motexafin gadolinium. Although in her experiments the maximum number of nuclei reached was only 15%, the difference can be explained by shorter exposure times (<48 hours), much lower exposure concentrations (25 μg/mL $\approx$ 17 μmol/L motexafin gadolinium compared with our 100 μmol/L), and possibly the use of a non–glioblastoma multiforme (murine sarcoma) cell line, although neither we nor others have adequately studied cell line variability regarding motexafin gadolinium uptake.

Tumor from motexafin gadolinium–treated animals has not yet been analyzed with subcellular resolution, and we cannot at this stage extrapolate that this drug reaches >90% cell nuclei *in vivo*. The previously analyzed compounds, Gd-DTPA and Gd-DOTA, did not reach the 90% uptake level either *in vitro* or *in vivo* (10). As reported in the same reference, if a compound does not reach 90% of the nuclei *in vitro*, it is unlikely to reach as many *in vivo*. It is also possible that in the *in vivo* situation, repetitive motexafin gadolinium administration will be necessary.

The present observation that motexafin gadolinium reaches >90% of the nuclei *in vitro* provides a basis for *in vivo* studies, which are currently under way. For the first GdSSR testing, orthotopic rodent models will be injected with motexafin gadolinium and then stereotactically irradiated at the European Synchrotron Radiation Facility in Grenoble. Because enhancement of double strand breaks with SSR and I or Pt has already been shown, we plan to proceed from the *in vitro* Gd localization directly to the *in vivo* GdSSR irradiation experiments.

Acknowledgments

We thank Angela Blissett for her collaboration.

References

1. Stupp R, van den Bent MJ, Hegi ME. Optimal role of temozolomide in the treatment of malignant gliomas. Curr Neurol Neurosci Rep 2005;5:198–206.
2. Estève F, Corde S, Elleaume H, Adam JF, et al. Enhanced radio sensitivity with iodinated contrast agents using monochromatic synchrotron X-rays on human cancerous cells. Acad Radiol 2002;9:S540–3.
3. Corde S, Joubert A, Adam JF, et al. Synchrotron radiation based experimental determination of the optimal energy for cell radiotoxicity enhancement following photoelectric effect on stable iodinated compounds. Br J Cancer 2004;91:544–51.
4. Biston MC, Joubert A, Adam JF, et al. Cure of Fisher rats bearing radioresistant F98 glioma treated with *cis*-platinum and irradiated with monochromatic synchrotron X-rays. Cancer Res 2004;64:2317–23.
5. Corde S, Balosso J, Elleaume H, et al. Synchrotron photoactivation of cisplatin elicits an extra number of DNA breaks that stimulate RAD51-mediated repair pathways. Cancer Res 2003;63:3221–7.
6. Adam JF, Elleaume H, Joubert A, et al. Synchrotron radiation therapy of malignant brain glioma loaded with an iodinated contrast agent: first trial on rats bearing F98 gliomas. Int J Radiat Oncol Biol Phys 2003;57:1413–26.
7. Adam JF, Joubert A, Biston MC, et al. Enhanced delivery of iodine for synchrotron stereotactic radiosurgery by means of intracarotid injection and blood brain barrier disruption. Int J Rad Oncol Biol Phys 2005;61:1173–82.
8. Adam JF, Joubert A, Biston MC, et al. Prolonged survival of Fischer rats bearing F98 glioma after iodine-enhanced synchrotron stereotactic radiotherapy. Int J Rad Oncol Biol Phys, in press 2005.
9. De Stasio G, Casalbore P, Pallini R, et al. Gadolinium in human glioblastoma cells for gadolinium neutron capture therapy. Cancer Res 2001;61:4272–7.
10. De Stasio G, Rajesh D, Casalbore P, et al. Are gadolinium contrast agents suitable for gadolinium neutron capture therapy? Neurol Res 2005;27:387–98.
11. ModyTD, Fu L, Sessler JL. Texaphyrins: synthesis and development of a novel class of therapeutic agents. In: Karlin KD, editor. Progress in inorganic chemistry. New York: John Wiley & Sons Inc; 2001. p. 551–98.
12. Sessler JL, Miller RA. Texaphyrins: new drugs with diverse clinical applications in radiation and photodynamic therapy. Biochem Pharmacol 2000;59:733–9.
13. Motexafin gadolinium: gadolinium (III) texaphyrin gadolinium texaphyrin Gd-Tex GdT2B2 PCI 0120. Drugs R D 2004;5:52–7.
14. Perez OD, Nolan GP, Magda D, et al. Motexafin gadolinium (Gd-Tex) selectively induces apoptosis in HIV-1 infected $CD4^+$ T helper cells. Proc Natl Acad Sci U S A 2002;99:2270–4.
15. Magda D, Lepp C, Gerasimchuk N, et al. Redox cycling by motexafin gadolinium enhances cellular response to ionizing radiation by forming reactive oxygen species. Int J Radiat Oncol Biol Phys 2001;51:1025–36.
16. Mehta MP, Shapiro WR, Glantz MJ, et al. Lead-in phase to randomized trial of motexafin gadolinium and whole-brain radiation for patients with brain metastases: centralized assessment of magnetic resonance imaging neurocognitive and neurologic end points. J Clin Oncol 2002;20:3445–53.
17. Young SW, Qing F, Harriman A. Gadolinium(III) texaphyrin: a tumor selective radiation sensitizer that is detectable by MRI. Proc Natl Acad Sci U S A 1996;93:6610–5.
18. Wu GN, Ford JM, Alger JR. The radiation enhancer motexafin gadolinium (MGd) does not penetrate the blood brain barrier in glioblastoma multiforme patients undergoing post-operative fractionated radiation therapy. Int J Radiat Oncol Biol Phys 2003;57:S329–30.
19. GoorleyT, Nikjoo H. Electron and photon spectra for three gadolinium-based cancer therapy approaches. Radiat Res 2000;154:556–63.
20. Powell CJ, Jablonski A. NIST electron inelastic-mean-free-path database, version 1.1. Gaithersburg (MD): National Institute of Standards and Technology; 2000.
21. Hall EJ. In: Radiobiology for the radiologist. 5th ed. Philadelphia: Lippincott Williams & Wilkins; 2000. p. 19–20.
22. Stein GH. T98G: an anchorage-independent human tumor cell line that exhibits stationary phase G1 arrest *in vitro*. J Cell Physiol 1979;99:43–54.
23. Haas-Kogan DA, Kogan SS, Yount G, et al. p53 function influences the effect of fractionated radiotherapy on glioblastoma tumors. Int J Radiat Oncol Biol Phys 1999;43:399–403.
24. Wang J, Hu L, Allalunis-Turner MJ, et al. Radiation-induced damage in two human glioma cell lines as measured by the nucleoid assay. Anticancer Res 1997;17:4615–8.
25. Falchetti ML, Pierconti F, Casalbore P, et al. Glioblastoma induces vascular endothelial cells to express telomerase *in vitro*. Cancer Res 2003;63:3750–4.
26. De Stasio G, Frazer BH, Girasole M, et al. Imaging the cell surface: argon sputtering to expose inner cell structures. Microsc Res Tech 2004;63:115–21.
27. Gilbert B, Perfetti L, Hansen R, et al. UV-ozone ashing of cells and tissues for spatially resolved trace element analysis. Front Biosci 2000;5:10–7.
28. Frazer BH, Girasole M, Wiese LM, et al. Spectromicroscope for the PHotoelectron Imaging of Nanostructures with X-rays (SPHINX): performance in biology medicine and geology. Ultramicroscopy 2004;99:87–94.
29. Frazer BH, Sonderegger BR, Gilbert B, et al. Mapping of physiological and trace elements with X-PEEM. J Phys Fr IV 2003;104:349–52.
30. Kilcoyne ALD, Tyliszczak T, Steele WF, et al. Interferometer-controlled scanning transmission X-ray microscopes at the Advanced Light Source. J Synchrotron Radiat 2003;10:125–36.
31. Tyliszczak T, Warwick T, Kilcoyne ALD, et al. Soft X-ray scanning transmission microscope working in an extended energy range at the advanced light source. In: Synchrotron Radiation Instrumention 2003, AIP Conference Proceedings. 2004;705:1356–9.
32. Woodburn KW. Intracellular localization of the radiation enhancer motexafin gadolinium using interferometric Fourier fluorescence microscopy. J Pharmacol ExpTher 2001;297:888–94.
33. Miles DR, Smith JA, Phan SC, et al. Population pharmacokinetics of motexafin gadolinium in adults with brain metastases or glioblastoma multiforme. J Clin Pharmacol 2005;45:299–312.
34. Hubbell JH. Photon cross sections attenuation coefficients, and energy absorption coefficients from 10 keV to 100 GeV. NSRDS-NBS 29. Gaithersburg (MD): National Bureau of Standards; 1969.